Noname manuscript No.
(will be inserted by the editor)

In-situ monitoring of FDM machine condition via acoustic emission

Haixi Wu · Yan Wang · Zhonghua Yu

Received: date / Accepted: date

Abstract Fused deposition modeling (FDM) is one of the most popular additive manufacturing technologies for fabricating prototypes with complex geometry and different materials. However, current commercial FDM machines have the limitations in process reliability and product quality. In order to overcome these limitations and increase the levels of machine intelligence and automation, machine conditions need to be monitored more closely as in closed-loop control systems. In this study, a new method for in-situ monitoring of FDM machine conditions is proposed, where acoustic emission (AE) technique is applied. The proposed method allows for the identification of both normal and abnormal states of the machine conditions. The time-domain features of AE hits are used as the indicators. Support vector machines with the radial basis function kernel are applied for state identification. Experimental results show that this new method can potentially serve as a non-intrusive diagnostic and prognostic tool for FDM machine maintenance and process control.

Keywords Fused deposition modeling · Additive manufacturing · Machine condition monitoring · Acoustic emission · Support vector machine

Haixi Wu
The State Key Laboratory of Fluid Power Transmission and Control, School of Mechanical Engineering, Zhejiang University, Hangzhou, Zhejiang, 310027, P.R. China

Yan Wang
Woodruff School of Mechanical Engineering, Georgia Institute of Technology, Atlanta, GA 30332, USA
Tel.: +1 404 894 4714
Fax: +1 404 894 9342
E-mail: yan.wang@me.gatech.edu

Zhonghua Yu
The State Key Laboratory of Fluid Power Transmission and Control, School of Mechanical Engineering, Zhejiang University, Hangzhou, Zhejiang, 310027, P.R. China

1 Introduction

The global market of additive manufacturing (AM) surpassed $3 billion in 2014, and its rapid growth is expected to continue over the coming years according to the 2014 Wohlers Report [58]. AM enables the flexibility for people to fabricate products, especially those with complex geometries. Users can fabricate products directly with various materials such as polymers [49], ceramics [56], and metals [35], etc. The basic principle of AM is that parts are made through adding materials by layers [16,33].

Among many AM techniques, fused deposition modeling (FDM) is popular because of its low cost. FDM is suitable for fabricating prototypes with thermoplastic materials such as acrylonitrile butadiene styrene (ABS), nylon, polylactic acid (PLA), and others. FDM can also print materials in a mixture or blended form [42,39]. However, the applications of FDM are still very limited because of the available material options as well as the quality of the built parts. The common quality issues include geometry deviations and cracks due to shrinkage [32,23], surface roughness [14,1], weak and anisotropic mechanical properties [49]. In order to increase the levels of machine intelligence and automation thus scale up the industrial and commercial applications of FDM with easy-to-use machines, it is also critical to implement process monitoring and control in commercial FDM machines. Currently they do not have closed-loop control systems and can suffer from breakdowns because of extruder blockage [34] and other failures without notice. Research efforts [44, 32] have been made to improve the design of FDM deposition mechanism to improve the quality of printed parts. Yet, the conditions of machines are not monitored during the fabrication process. A cost-effective and efficient closed-loop system with the capabilities of sensing, information processing, and feedback for adjustment will be necessary to improve the reliability and usability of machines thus the repeatability of products. Although plenty of research work (e.g. [3,53,52]) has been done for product monitoring during fabrication, to the authors' knowledge, there is still no study of FDM machine condition monitoring.

A complete AM process typically consists of many iterations of multi-step procedures such as nozzle position adjustment, material deposition, preheating, melting, cooling, or chemical curing in the layer-by-layer construction scheme. If each step during the process corresponds to a machine state, FDM machines experience state transitions much more frequently than those used in traditional subtractive manufacturing processes. Monitoring the condition of FDM machines in situ at each of these steps and preventing print failures in the relatively long fabrication process help reduce waste and ensure the quality of final products. Important FDM machine states need to be identified to keep track of the conditions, such as the ones shown in Fig. 1, including both normal and abnormal states. The circles in the figure represent states, whereas arrows indicate state transitions. The normal states are material loading, normal extruding, and idle. The abnormal states include the ones that run out of material, extruder semi-blocked with chatter and uneven extrusion due to

breakdown of heater, low-quality filament, extruder wear, or working environment contamination, as well as total blockage without extrusion completely.

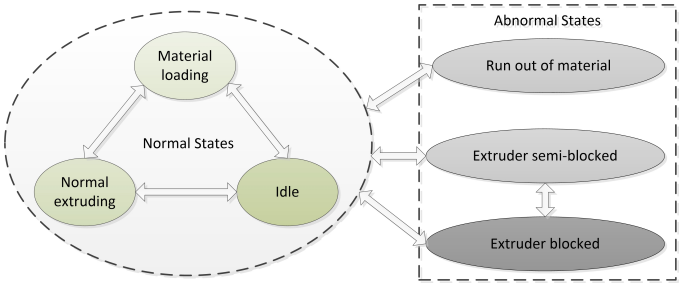

Fig. 1 Important states of FDM machine conditions during fabrication process

The objective of this research is to develop a non-intrusive approach for in-situ monitoring of FDM machine conditions, in order to detect and prevent major breakdowns and process failures. The overall goal is to achieve better process reliability, repeatability, and automation of FDM. In particular, the focus of this study is on monitoring the conditions of FDM machine extruder. The extruder is one of the most critical components in FDM machines that have significant influence on the overall product quality. Several key process parameters that affect the overall product quality [49], such as bead width, air gap, and build environment temperature, are all related to the extruder's operating condition. For example, the blockage of the extruder will result in a different bead width from the regular one. The air gap will also be changed and further affect the filling path and filling rate, given that the printing path and speed are predetermined when there is no feedback control for in-time adjustment.

In the proposed approach for in-situ monitoring, acoustic emission (AE) technique is applied to monitor FDM machine condition for the first time. There are three major reasons of using AE sensor in this study. First, AE signal contains rich information of the fabrication process. Information in both time and frequency domains of the AE signals can be processed and analyzed efficiently in real-time. Second, the sources of AE signals are the running machine itself. No external stimulation or sources are needed, which simplifies the set up of the monitoring system. Last but not the least, AE technology is non-intrusive. This means that the AE sensor can be attached to the FDM machine. During the fabrication process, AE data collected from the FDM machine extruder are analyzed. Important information of AE hits are collected and identified as features. Support vector machine (SVM) is applied to recognize machine states from features. This approach can potentially serve as a diagnostic and prognostic tool for FDM machine maintenance and process control.

In the remainder of this paper, an overview of relevant work is given in Section 2. In Section 3, the related methodologies and experimental set up are

described. The results of experiments and SVM-based state identifications are discussed in Section 4.

2 Background

2.1 Machine condition and process monitoring

Machine condition monitoring has played a very important role in modern manufacturing because it can significantly improve the reliability, increase the level of automation, and reduce the total maintenance costs [24]. Machine condition monitoring has been extensively studied in traditional machining process [50]. Based on the information collected from the process, machine states can be acquired and the trend of operation conditions can be predicted. The typical machine condition monitoring sequence includes process variable selection, sensing and data collection, data processing and feature extraction, cognitive decision making, and action [50]. Currently, many machine condition monitoring strategies are based on two types of models, physics-based models and data-driven (empirical) models [19]. The first type of models predict the phenomena of systems with the consideration of physical natures and mechanisms of the systems, whereas the second type utilize historical data only to build analytical models for product property or failure predictions.

In the domain of FDM process many efforts have also been made to improve the part quality. Some physics-based models have been developed [51, 1,7,4,26]. However, to date, it is still a very challenging task to build accurate physical models because it requires in-depth knowledge of FDM process and many factors can affect the model accuracy, such as anisotropic material properties [49,63], fatigue effects [31], etc. Given the limitations, researchers also employed experiment-based empirical modeling approaches [46,47,45,14, 38,28]. Sensing techniques have also been used to ensure the quality of FDM built parts [40,27,11,41].

The above studies focused on the fabricated parts and fabrication process at the normal working status, but not the influences of machine conditions. In the present work, a new in-situ machine condition monitoring method based on AE signals is proposed in an attempt to fill this gap.

2.2 Acoustic Emission (AE)

AE sensors detect the stress waves generated from the source of emission, such as crack, friction, and deformation. A wide range of frequency spectra generated by different sources can be detected simultaneously by AE sensors. AE signals can be used to identify system dynamics, material flows, and other machine statuses.

Usually an AE sensor is attached to the surface of equipment to collect signals. Vacuum grease or magnetic holder is often used for better signal

transmission. The collected signals will then be further amplified, filtered, and processed by a preamplifier and a data acquisition system before stored in a computer. AE signals contain rich information of the on-going process as well as interfering noises. Using differential AE sensors, setting up floating threshold, and applying signal processing techniques are common methods to remove noises [30,17,61,37].

AE has been widely applied as a non-destructive and non-intrusive monitoring technique for manufacturing processes [12], including tool wear identification [10], machining workpiece defect monitoring [60], and machine component defect detection [25], as well as coating [36], granulation [5], and crystallization [15] in chemical processing.

Extensive literature consultation suggests that AE technique has not been applied to FDM machine condition monitoring. Thus, in this study, AE is applied to detect both normal and abnormal states of FDM machine conditions.

3 Methodologies and experimental set up

3.1 AE signal processing and important features

In a more efficient way, AE signal can be stored as a series of hits, instead of as the original signal data. An AE hit refers to the process of detecting an AE event. Several important features are used to describe the measurable characteristics of AE hits. Fig. 2 illustrates an example of an AE hit and the related features. The features include amplitude, counts, and duration. The set of AE features can be computed and used to describe the characteristics of an AE signal. The features are calculated as follows.

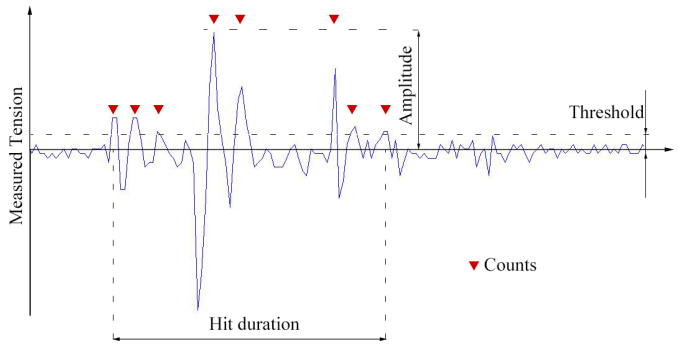

Fig. 2 A typical AE hit and the related features

Amplitude (A) is a very important feature of AE. This feature is the peak voltage of the wave within an AE hit. Usually the amplitude of an AE hit is

expressed on a decibel (dB) scale as:

$$A = 20log(\frac{U_{max}}{U_{ref}}) \tag{1}$$

where U_{max} is the peak voltage and U_{ref} is the reference voltage in the scale of mV. Counts are the numbers of pulses that cross a predefined threshold. Duration describes the elapsed time from the first count to the last one in one AE hit.

Other features that can be obtained, including peak frequency (P-Freq), frequency centroid (Freq-C), root mean square (RMS), absolute energy (ABS-Energy), and cumulative absolute energy (C-ABS-Energy). P-Freq is the point in the power spectrum with maximum magnitude and Freq-C is the barycentre of an AE hit's power spectrum. RMS is a feature used to describe the strength of AE signal in time domain. RMS is defined as:

$$AE_{RMS} = \sqrt{\frac{1}{t_2 - t_1}\int_{t_1}^{t_2} u(t)^2 dt} \tag{2}$$

where $u(t)$ is the output voltage of AE sensor. ABS-Energy is defined as

$$E_{ABS-Energy} = \alpha \int u(t)^2 dt \tag{3}$$

which is the integration of the output voltage $u(t)$ of the sensor, where α is inversely proportional to the electrical resistance of the sensor. ABS-Energy is also an important feature to describe the strength of an AE hit. C-ABS-Energy of n AE hits can be attained as the sum of ABS-Energy, i.e.

$$E_{C-ABS-Energy} = \sum_{i=1}^{n} E_{ABS-Energy}^{(i)} \tag{4}$$

3.2 Support Vector Machine (SVM)

In this study, SVM [54,55] is adopted to identify FDM machine conditions. SVM has been generally accepted as a useful machine learning technique for feature identification and classification problems. It has been widely applied in manufacturing system monitoring [9,48,57,62].

SVM is basically a binary classification tool. However, in this study, multiple classes need to be identified by using SVMs. There are three common solutions for this particular situation: one-against-one, one-against-all, and directed acyclic graph SVM [20]. One-against-one is selected in this study because it is the best in general with the consideration of accuracy and training time [20]. Radial basis function (RBF) kernel is also applied. Keerthi and Lin [29] pointed out that RBF is superior to the linear kernel after parameters are selected. The RBF kernel can handle cases through the nonlinear mappings of the input data into a higher dimensional space and then searching a linear

separating hyperplane with the maximum margin. In addition, RBF has fewer hyper-parameters and numerical difficulties than other kernels such as polynomial kernel and sigmoid kernel. The RBF kernel is suitable in this study also because the number of input features is limited. ABS-Energy and its standard deviation (STD) are selected as the two input feature vectors. In this study, all SVMs were constructed using LIBSVM [6] toolbox in a MATLAB environment.

3.3 FDM machine and AE system set up

The FDM machine used in this study is Model E5 Engine made by HYREL3D. The extruder used in this study is MK-1 hot-heated filament extruder and the material is ABS.

The AE system includes the senor, preamplifier, and data acquisition system. The AE sensor used in the experiments is Model MD made by Mistragroup. This differential sensor can eliminate some background noises. Approximately 2dB tune of noise improvement can be achieved compared to a single-end sensor. This sensor has the operating frequency response within the range of 100-900kHz, and the temperature range is between $-65°C$ to $177°C$. The original AE signal is conditioned and amplified by a PAC 2/4/6 preamplifier, then received and processed by a PAC PCI-2 fast data acquisition (DAQ) system. The PAC PCI-2 system has a 18-bit A/D conversion scheme with the sampling rate up to 40M samples per second. It has an on-board digital signal processing (DSP) module so that real-time signal processing performance can be achieved. A schematic drawing of the experimental set-up is shown in Fig 3. The AE sensor was securely attached on the side surface of the extruder with vacuum grease. The sampling rate was set to 5M samples per second in order to obtain a balance between the information integrity and real time performance.

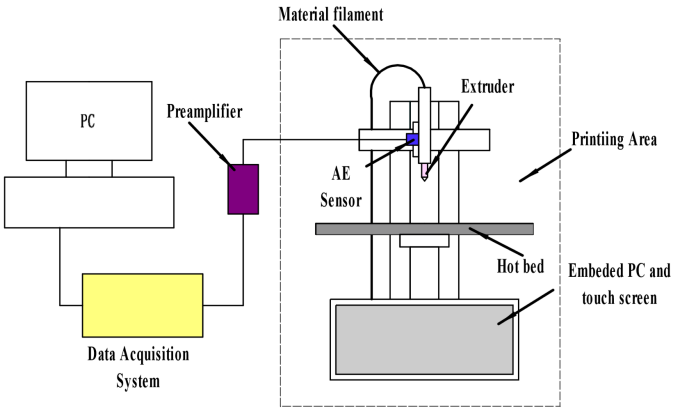

Fig. 3 The schematic drawing of experimental set up

3.4 Experimental procedures

By taking the advantages of the AE system, the relationship between the machine conditions and the features of AE hits can be investigated in details.

The first experiment was carried out to identify the sensitive features of the emitted AE signals from the FDM machine extruder. Two normal states of extruder operating conditions were included in the process. The nozzle of extruder was heated to a temperature of 230°C. In the material loading state, the material filament was loaded into the extruder without printing. In the normal extruding state, the material was extruded at the normal printing speed. In order to eliminate the background noises from motor rotation and component movement, AE hits were collected with only the extruder being operated.

In the second experiment, a common failure mode because of the running out of material during the extruding process was studied. A short segment of filament was used when the FDM machine was operated at a normal extruding condition. After this short segment ran out, the FDM machine extruder switched to a different condition of extruding without material. The state transition from the normal extruding to the extruding without material was created intentionally. The AE hits during this process were recorded and analyzed.

To further show the feasibility of the proposed approach and investigate another common failure of FDM machines, an experiment of detecting three extruding states (normal, semi-blocked, and blocked) was also conducted. A semi-blocked state refers to a condition that the extruder cannot extrude materials as smoothly as in the normal extruding state. Both the chatter of the extruder and the unevenly extruded materials can be seen. The causes of this condition could be the blockage of the extruder by contamination, extruder wear, low-quality filament, the sudden breakdown of heater on the extruder, etc. A blocked state refers to a condition that the extruder is totally blocked and no material can be extruded. In this experiment, the three extruding states were created intentionally by modifying the heating temperature of the extruder. In the normal extruding state, the heating temperature was 230°C, whereas the temperatures of the semi-blocked and blocked states were 180°C and 130°C respectively. The AE hits from the above three extruding states were recorded and analyzed.

4 Results and discussions

The results of the above three experiments are reported in Sections 4.1, 4.2, and 4.3 respectively.

4.1 The study of two normal states

Fig. 4 shows the simultaneous features of AE hits recorded in the first experiment, including ABS-Energy, counts, RMS, Freq-C, and P-Freq. State 1 is the material loading state, whereas State 2 is the normal extruding state. The AE hits located between State 1 and State 2 were collected from the background electrical noises because mechanical movement was avoided. The features of AE hits were calculated directly by the PAC PCI-2 system. All of these features were obtained in real time.

The features in the frequency domain were analyzed. As shown in Figs. 4(d) and (e), the majority of the frequency features, i.e. Freq-C and P-Freq, are located in the range between 50 and 300 KHz. In particular, the AE hits recorded as electrical noises between State 1 and State 2 can help identify the dominant frequency components of the background noises. In order to obtain the information of frequency range changes along time, the short-time fast Fourier transform (ST-FFT) was also employed. Fig. 5 depicts the result of ST-FFT analysis for an AE hit segment. From Fig. 5, one can also tell that most of the frequency components fall into the range below $333KHz$, which is consistent with the results in Fig. 4. However, the differences of the frequency features between State 1 and State 2 are not obvious.

The features in the time domain were also calculated, including ABS-Energy, counts, and RMS. As shown in Figs.4(a), (b), and (c), the differences between State 1 and State 2 are obvious, including the maximum values and the distributions. In State 1, most of the ABS-Energy values are less than 25,000 aJ, with one outlier reaching 90,000 aJ mostly as a result of system noise. In State 2, the maximum value of ABS-Energy is above 100,000 aJ, and the mean value is also higher than the one in State 1. It suggests that the values of ABS-Energy can be used as the indicator of different states. The ABS-Energy of background noise between State 1 and State 2 remains at a low level of about 200 aJ. The changes of counts between two states for AE counts is similar to the ABS-Energy. It is because the more counts that a signal crosses the threshold within a hit, the more energy this hit contains. The RMS values of AE hits also show a very similar trend.

It is seen that the time-domain features are more sensitive to the state transition than the frequency features through this experiment. In other words, the ABS-Energy, counts, and RMS of AE hits are more directly related to the working conditions of FDM machine extruder. Additional signal processing tools such as wavelet transform and Hilbert-Huang transform (HHT) analyses are needed to discover the relations between frequency features and machine states in-depth other than only centroids and peaks. Wavelet transform is one of the classical and widely used time-frequency analysis tool for non-stationary signals in manufacturing process monitoring [8, 13, 59]. Similarly, HHT performs time-frequency-energy analysis based on empirical mode decomposition and Hilbert spectral analysis for non-stationary signals [21, 22]. However, when the amount of data is large, such as in this study where hundreds of AE hits were recorded per second, these signal processing tools have limitations for

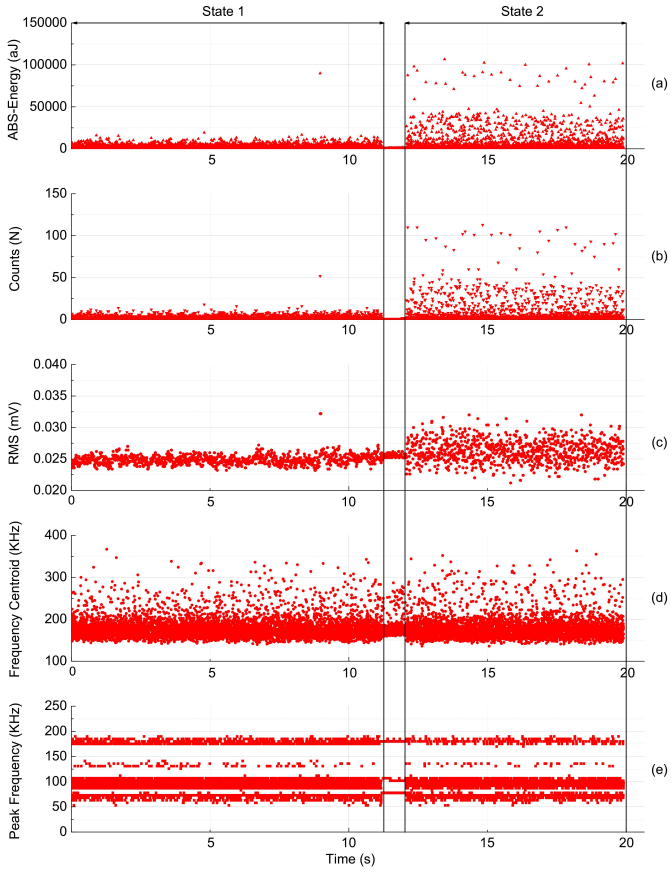

Fig. 4 Simultaneous features of AE hits during state transition

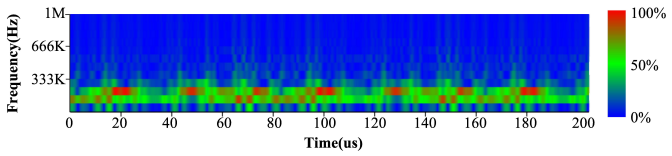

Fig. 5 A demonstration of ST-FFT analysis of an AE hit segment

real-time applications. Therefore we chose the time-domain features to identify different states in the subsequent studies.

4.2 The study of run-out-of-material state

4.2.1 Experiment and AE data analysis

Based on the results in Section 4.1, only the time-domain features were focused here. Fig. 6 shows three features of AE hits recorded from the second experiment, which are ABS-Energy, RMS, and corresponding C-ABS-Energy.

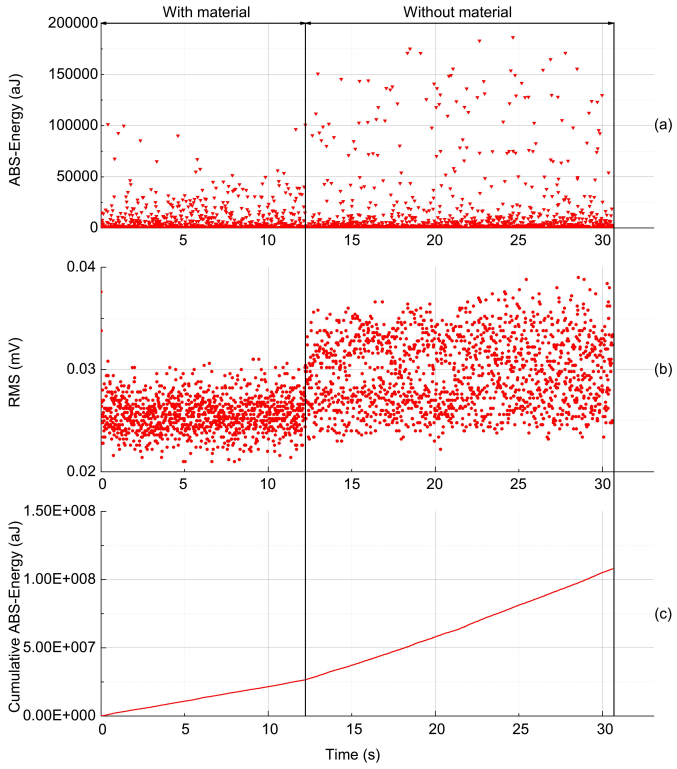

Fig. 6 Features of AE hits during state transition of sudden running out of material

In the first state, when the extruder was operated with material, the maximum value of ABS-energy remained around 100,000 aJ, and the values of RMS are mostly within the range from 0.02 to $0.03mV$, as shown in Fig. 6(a) and (b). In the second state after the material runs out, the maximum value of ABS-Energy increases to a higher level of 200,000 aJ. A significant increase of RMS values can also be seen in Fig. 6(b). The results were consistent with the observations from other work [43, 15, 18, 2] where the energy level and RMS value of AE signal were applied as the machine condition indicators of other manufacturing systems. Fig. 6(c) shows a line plot of C-ABS-Energy during this transition period. The slope of the second state is larger than the one in

the first state. A detailed comparison of the means and standard deviations of AE features between the two states is presented in Table.1.

Table 1 Means and standard deviations of ABS-Energy and RMS

		With material	Without material
ABS-Energy	Mean value (aJ)	4588.08	9270.82
	STD	10560.51	25973.94
RMS	Mean value (mV)	0.0256	0.0296
	STD	0.0018	0.0034

4.2.2 Two-state identification based on SVM

The two states, extruding with and without material, were identified based on SVM with the collected data. A total of 14,544 AE hits were recorded in 33 seconds. The AE hits were separated into 66 segments. Thus approximately 220 AE hits were located in each segment. The duration of each segment was 500 microseconds (ms). According to the analysis in Section 4.2.1, the means and standard deviations of ABS-Energy are strongly correlated with the two states. Therefore, the two statistical measures for each segment were calculated and used as the input feature vectors for SVM. The values were normalized to the range of $[0, 1]$ in order to improve the accuracy of SVM. Fig. 7 shows the results of the normalized means and standard deviations of ABS-Energy for the 66 AE segments.

With the above analysis, SVM was then applied for state identification. A grid search was used in order to find out an appropriate set of parameters for the RBF kernel (C, γ), where C is the penalty parameter and γ can be considered as the inverse of the radius of data sample's influence. The values of the parameters were selected as $C = 2$ and $\gamma = 2$ respectively in this experiment. A cross-validation method was applied to test the SVM and prevent the over-fitting problem. Half of the segments were used for training, and the other half were for validation.

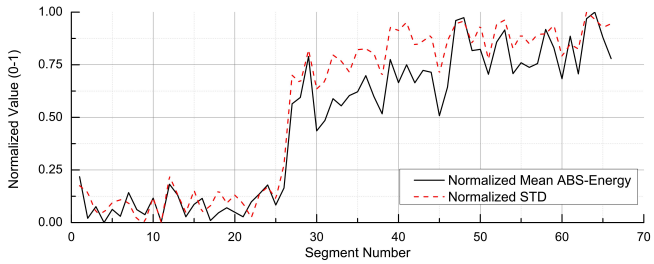

Fig. 7 Segment analysis of ABS-Energy

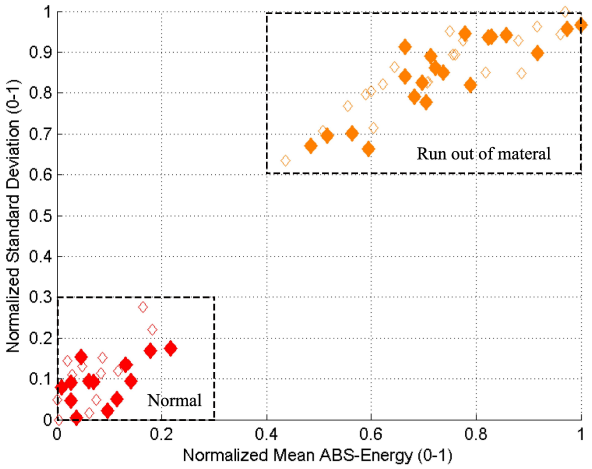

Fig. 8 SVM cross-validation result for two-state identification

Fig. 8 shows the cross-validation result of the SVM. The unfilled markers represent the segments from the training set. The filled markers represent those from the test set. The cross-validation results showed that an accuracy rate of 100% was achieved. With the trained parameters, the same construction of SVM was used to test the whole data segments. After another round of training with all of the 66 data segments, the predicted state labels and actual state labels were compared again. The accuracy rate was also 100%. All segments were correctly classified. There is no overlap between the two sets of data samples, and a clear boundary is observed. The results indicate that the state transition from the normal extruding to a sudden run out of materials can be monitored with the proposed approach during the FDM fabrication process.

4.3 Extruder blockage detection

4.3.1 Experiment and AE data analysis

The results in Section 4.2.2 suggest that the mean value and the distribution of ABS-Energy can be applied as the characteristic features for FDM extruder condition monitoring. The third experiment for extruder blockage detection was further conducted and the results are discussed here. As an illustration, Fig. 9 shows an example of a typical extruder blockage. It is seen that the filament below the feeding gear was fractured and distorted so that the upper part of filament can no longer be fed in.

Fig. 10 displays the recorded ABS-Energy of AE hits from the three different extruding states (normal, semi-blocked, and blocked). The respective means and standard deviations are shown in Table 2.

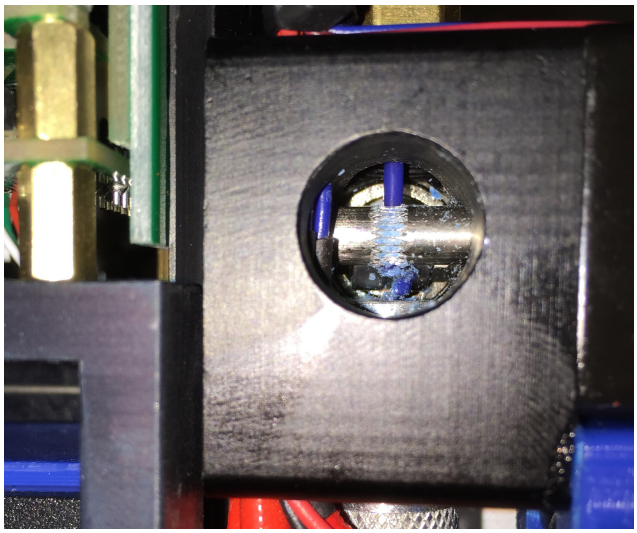

Fig. 9 A typical extruder blockage

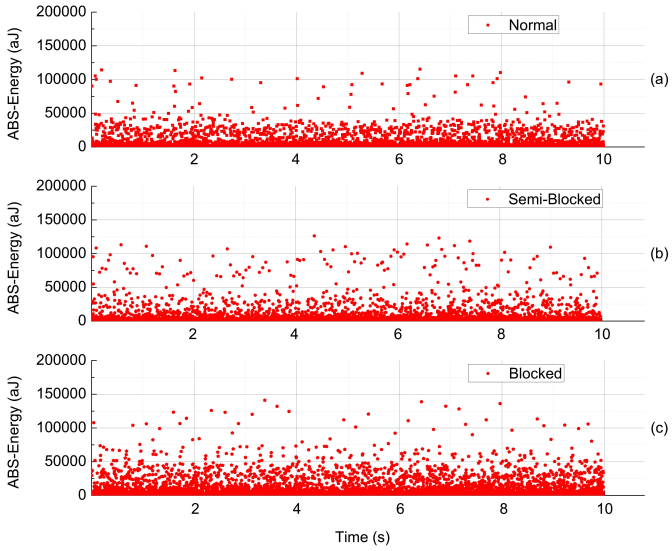

Fig. 10 ABS-Energy of AE hits from three different extruding states

Table 2 Means and standard deviations of ABS-Energy from three different extruding states

		Normal	Semi-Blocked	Blocked
ABS-Energy	Mean Value (aJ)	4751.86	5438.59	8313.59
	STD	9008.07	12391.49	14788.39

4.3.2 Multi-state identification based on SVM

Similar to the analysis in Section 3.2, one-against-one SVM with the RBF kernel was chosen for multi-state identification. A similar segment treatment was also applied to AE hits collected at the three different extruding states separately. Each set of data was divided into 20 segments with a duration of approximately 500ms. A total of 60 segments were generated in this experiment. Then the mean value of ABS-Energy as well as its standard deviation for each segment were calculated. The results were also normalized before the SVM is applied. The RBF parameters $C = 2$ and $\gamma = 20$ were selected in this case after the grid-searching method was applied.

Fig. 11 displays the cross-validation result. According to the cross-validation results of the multi-state identification, an accuracy rate of 95% was achieved, where 29 out of 30 segments were successfully classified. The same SVM parameters were used again to test all of the 60 data segments. After the training of the SVM with all segments was finished, the predicted state labels and the actual state labels were compared and the accuracy rate reached 97%. A total of 58 out of 60 segments were correctly classified. Compared to the two-state identification in Section 4.2.2, the accuracy rate is slightly dropped in this experiment, mostly because the number of states is increased and the samples are more dispersed. Thus it is more difficult for SVM to define the boundaries among these three states. Nevertheless, the accuracy rate in this case is high enough for robust prediction. Thus the proposed approach is very likely to correctly detect extruder blockage during the FDM machine operation in real time.

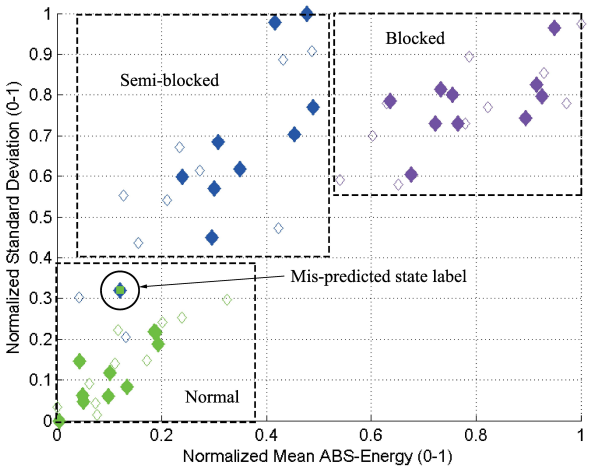

Fig. 11 Cross-validation result of SVM: The unfilled markers represent segments from the training set; The filled markers represent segments from the test set; The filled marker with a square inside represents the mis-predicted state label assigned by the SVM.

4.4 FDM machine condition monitoring with all states

In order to estimate the capacity of the proposed method for the overall machine condition monitoring, SVM is further applied to identify all of the above five states, which are material loading, normal extruding, run out of material, semi-blocked, and blocked states respectively. The AE data from material loading (Section 4.1) and run out of material (Section 4.2) for a period of 10 seconds were combined with the data in Section 4.3 for the five-state identification study. In this analysis, data samples from each state were separated into 20 segments with a duration of 500ms. A total of 100 segments were generated. Again, the mean and standard deviation of ABS-Energy for each segment were calculated and linearly scaled to the range of [0,1]. The RBF parameters were $C = 20$ and $\gamma = 20$.

The cross-validation result is shown in Fig. 12. With the five states combined, the accuracy rate of prediction in cross-validation was dropped to 92%, where 4 out of 50 samples were mis-predicted by the SVM. The overall accuracy rate with all 100 segments was 95%.

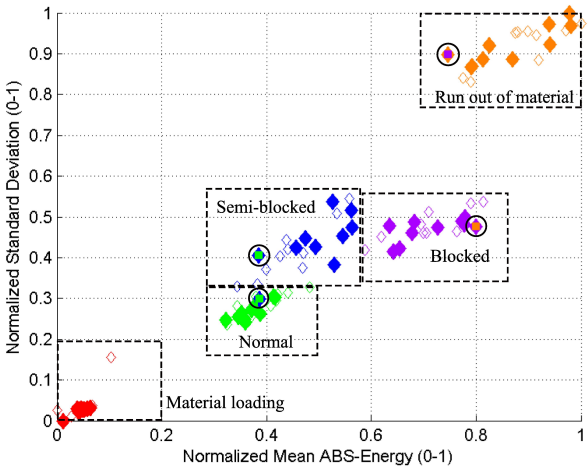

Fig. 12 Cross-validation result of SVM for five states: The unfilled markers represent segments from the training set; The filled markers represent segments from the test set; The filled markers with squares inside represent the mis-predicted state labels assigned by the SVM

From the comparison between the result of the five-state identification and the results in Sections 4.2 and 4.3, one may conclude that more states lead to lower accuracy of SVM classification. There are three major reasons for this. First, SVMs are for binary classification in nature instead of multiple states. This may affect the accuracy of the constructed SVM. Other multiclass classification methods need to be applied to overcome this limitation. Second, only two AE features (mean and standard deviation of ABS-Energy) were used

as the input feature vectors of SVM in this study. Thus, the distribution of the samples from different states is limited in a two-dimensional space. Overlaps occur if the distributions of the data samples from different groups are close to each other in this two-dimensional space. In this case, it would be difficult for a SVM to find the separating boundaries among these overlapped data samples. Higher-dimensional feature vectors are needed in order to improve the accuracy of prediction. Third, because of the measurement uncertainties in the recorded AE data, the selected duration of each data segment will also affect the accuracy. In this study, 500ms was chosen as the duration. Shorter time windows tend to result in lower accuracies.

5 Concluding remarks

In this paper, a non-intrusive condition monitoring method for FDM machines based on AE sensing techniques was presented. Time-domain features of AE hits were used to identify five different extruder operating conditions of FDM machine. The features are ABS-Energy, counts, and RMS of AE hits. The means and standard deviations of ABS-Energy were applied in the SVM classification. Three experimental studies were carried out. Both normal and abnormal states were identified. The experimental results suggest that AE technique can provide a good approach to monitor FDM processes in-situ with the advantages of non-intrusiveness and ease of computation.

Further investigation of choosing high-dimensional AE features is needed for better accuracy of SVM prediction and machine state identification. Multi-class classification algorithms other than SVMs can also be chosen. System background noises also affect the accuracy of predication. They need to be efficiently identified and filtered out particularly in the cases when both mechanical and electrical background noises are present. It is also important to point out that several time-domain AE features such as ABS-Energy and RMS are very sensitive to the location of the AE sensor installation. Thus the process of normalization is critical to eliminate this scaling problem. The signal-noise ratio is also dependent on the location of the AE sensor and the distance between the AE source and the sensor. How to improve the signal-noise ratio requires further studies.

Acknowledgements This research is supported in part by China Scholarship Council with a scholarship (No. 201406320108) to the first author. The authors would like to thank Dr. Bin He of Shanghai University for discussions.

References

1. Ahn, D., Kweon, J.H., Kwon, S., Song, J., Lee, S.: Representation of surface roughness in fused deposition modeling. Journal of Materials Processing Technology **209**(1516), 55935600 (2009). DOI 10.1016/j.jmatprotec.2009.05.016. 00049

2. Arul, S., Vijayaraghavan, L., Malhotra, S.K.: Online monitoring of acoustic emission for quality control in drilling of polymeric composites. Journal of Materials Processing Technology **185**(13), 184190 (2007). DOI 10.1016/j.jmatprotec.2006.03.114. 00025
3. Bikas, H., Stavropoulos, P., Chryssolouris, G.: Additive manufacturing methods and modelling approaches: a critical review. The International Journal of Advanced Manufacturing Technology p. 117 (2015). DOI 10.1007/s00170-015-7576-2
4. Boschetto, A., Bottini, L.: Roughness prediction in coupled operations of fused deposition modeling and barrel finishing. Journal of Materials Processing Technology **219**, 181192 (2015). DOI 10.1016/j.jmatprotec.2014.12.021. 00000
5. Briongos, J.V., Sobrino, C., Gmez-Hernndez, J., Santana, D.: Characterization of flow-induced vibrations in gassolid fluidized beds: Elements of the theory. Chemical Engineering Science **93**, 181196 (2013). DOI 10.1016/j.ces.2013.01.056. 00004
6. Chang, C.C., Lin, C.J.: LIBSVM: A library for support vector machines. ACM Transactions on Intelligent Systems and Technology **2**, 27:1–27:27 (2011). Software available at http://www.csie.ntu.edu.tw/ cjlin/libsvm
7. Chang, D.Y., Huang, B.H.: Studies on profile error and extruding aperture for the RP parts using the fused deposition modeling process **53**(9), 1027–1037 (2010-08-15). DOI 10.1007/s00170-010-2882-1. URL http://link.springer.com/article/10.1007/s00170-010-2882-1. 00000
8. Chen, B.H., Wang, X.Z., Yang, S.H., McGreavy, C.: Application of wavelets and neural networks to diagnostic system development, 1, feature extraction. Computers & Chemical Engineering **23**(7), 899906 (1999). DOI 10.1016/S0098-1354(99)00258-6. 00082
9. Chinnam, R.B.: Support vector machines for recognizing shifts in correlated and other manufacturing processes. International Journal of Production Research **40**(17), 44494466 (2002). DOI 10.1080/00207540210152920. 00049
10. Dolinek, S., Kopa, J.: Acoustic emission signals for tool wear identification **225229, Part 1**, 295–303 (1999). DOI 10.1016/S0043-1648(98)00363-9. URL http://www.sciencedirect.com/science/article/pii/S0043164898003639
11. Domingo-Espin, M., Borros, S., Agullo, N., Garcia-Granada, A.A., Reyes, G.: Influence of building parameters on the dynamic mechanical properties of polycarbonate fused deposition modeling parts. 3D Printing and Additive Manufacturing **1**(2), 7077 (2014). DOI 10.1089/3dp.2013.0007. 00001
12. Dornfeld, D.: Application of acoustic emission techniques in manufacturing. NDT & E International **25**(6), 259269 (1992). DOI 10.1016/0963-8695(92)90636-U. 00054
13. Fang, N., Pai, P.S., Mosquea, S.: Effect of tool edge wear on the cutting forces and vibrations in high-speed finish machining of inconel 718: an experimental study and wavelet transform analysis. The International Journal of Advanced Manufacturing Technology **52**(1-4), 6577 (2011). DOI 10.1007/s00170-010-2703-6. 00014
14. Garg, A., Tai, K., Lee, C.H., Savalani, M.M.: A hybrid m5 -genetic programming approach for ensuring greater trustworthiness of prediction ability in modelling of fdm process. Journal of Intelligent Manufacturing **25**(6), 13491365 (2014). DOI 10.1007/s10845-013-0734-1. 00000
15. Gherras, N., Serris, E., Fevotte, G.: Monitoring industrial pharmaceutical crystallization processes using acoustic emission in pure and impure media. International Journal of Pharmaceutics **439**(12), 109119 (2012). DOI 10.1016/j.ijpharm.2012.09.048. 00009
16. Gibson, I., Rosen, D.W., Stucker, B.: Additive Manufacturing Technologies. Springer US (2010). URL http://link.springer.com/10.1007/978-1-4419-1120-9. 00375
17. Gowid, S., Dixon, R., Ghani, S.: A novel robust automated fft-based segmentation and features selection algorithm for acoustic emission condition based monitoring systems. Applied Acoustics **88**, 6674 (2015). DOI 10.1016/j.apacoust.2014.08.007. 00000
18. Han, X., Wu, T.: Analysis of acoustic emission in precision and high-efficiency grinding technology. The International Journal of Advanced Manufacturing Technology **67**(9-12), 19972006 (2013). DOI 10.1007/s00170-012-4626-x. 00000
19. Heng, A., Zhang, S., Tan, A.C.C., Mathew, J.: Rotating machinery prognostics: State of the art, challenges and opportunities. Mechanical Systems and Signal Processing **23**(3), 724739 (2009). DOI 10.1016/j.ymssp.2008.06.009. 00401
20. Hsu, C.W., Lin, C.J.: A comparison of methods for multiclass support vector machines. IEEE Transactions on Neural Networks **13**(2), 415425 (2002). DOI 10.1109/72.991427. 05208

21. Huang, N.E., Shen, Z., Long, S.R., Wu, M.C., Shih, H.H., Zheng, Q., Yen, N.C., Tung, C.C., Liu, H.H.: The empirical mode decomposition and the Hilbert spectrum for nonlinear and non-stationary time series analysis, vol. 454, p. 903995. The Royal Society (1998). URL http://rspa.royalsocietypublishing.org/content/royprsa/454/1971/903.full.pdf. 00002
22. Huang, N.E., Wu, Z.: A review on hilbert-huang transform: Method and its applications to geophysical studies. Reviews of Geophysics **46**(2), RG2006 (2008). DOI 10.1029/2007RG000228. 00472
23. Huang, Q., Zhang, J., Sabbaghi, A., Dasgupta, T.: Optimal offline compensation of shape shrinkage for three-dimensional printing processes. IIE Transactions **47**(5), 431441 (2015). DOI 10.1080/0740817X.2014.955599
24. Jardine, A.K.S., Lin, D., Banjevic, D.: A review on machinery diagnostics and prognostics implementing condition-based maintenance **20**(7), 1483–1510 (2006-10). DOI 10.1016/j.ymssp.2005.09.012. URL http://www.sciencedirect.com/science/article/pii/S0888327005001512. 01398
25. Jian, H., Lee, H.R., Ahn, J.H.: Detection of bearing/rail defects for linear motion stage using acoustic emission **14**(11), 2043–2046 (2013-11-01). DOI 10.1007/s12541-013-0256-y. URL http://link.springer.com/article/10.1007/s12541-013-0256-y. 00000
26. Jin, Y.a., He, Y., Xue, G.h., Fu, J.z.: A parallel-based path generation method for fused deposition modeling. The International Journal of Advanced Manufacturing Technology **77**(5-8), 927937 (2014). DOI 10.1007/s00170-014-6530-z. 00000
27. Kantaros, A., Karalekas, D.: Fiber bragg grating based investigation of residual strains in ABS parts fabricated by fused deposition modeling process **50**, 44–50 (2013-09). DOI 10.1016/j.matdes.2013.02.067. URL http://www.sciencedirect.com/science/article/pii/S0261306913001787. 00006
28. Karamooz Ravari, M.R., Kadkhodaei, M., Badrossamay, M., Rezaei, R.: Numerical investigation on mechanical properties of cellular lattice structures fabricated by fused deposition modeling. International Journal of Mechanical Sciences **88**, 154161 (2014). DOI 10.1016/j.ijmecsci.2014.08.009. 00001
29. Keerthi, S.S., Lin, C.J.: Asymptotic behaviors of support vector machines with gaussian kernel. Neural Computation **15**(7), 16671689 (2003). DOI 10.1162/089976603321891855. 01127
30. Kim, J.S., Kang, M.C., Ryu, B.J., Ji, Y.K.: Development of an on-line tool-life monitoring system using acoustic emission signals in gear shaping. International Journal of Machine Tools and Manufacture **39**(11), 17611777 (1999). DOI 10.1016/S0890-6955(99)00030-9. 00025
31. Lee, J., Huang, A.: Fatigue analysis of fdm materials. Rapid Prototyping Journal **19**(4), 291299 (2013). DOI 10.1108/13552541311323290. 00001
32. Lee, W.c., Wei, C.c., Chung, S.C.: Development of a hybrid rapid prototyping system using low-cost fused deposition modeling and five-axis machining. Journal of Materials Processing Technology **214**(11), 23662374 (2014). DOI 10.1016/j.jmatprotec.2014.05.004. 00003
33. Levy, G.N., Schindel, R., Kruth, J.P.: RAPID MANUFACTURING AND RAPID TOOLING WITH LAYER MANUFACTURING (LM) TECHNOLOGIES, STATE OF THE ART AND FUTURE PERSPECTIVES **52**(2), 589–609 (2003). DOI 10.1016/S0007-8506(07)60206-6. URL http://www.sciencedirect.com/science/article/pii/S0007850607602066. 00370
34. Mohd Halidi, S.N.A., Abdullah, J.: Moisture and humidity effects on the abs used in fused deposition modeling machine. Advanced Materials Research **576**, 641644 (2012). DOI 10.4028/www.scientific.net/AMR.576.641
35. Murr, L.E., Gaytan, S.M., Ramirez, D.A., Martinez, E., Hernandez, J., Amato, K.N., Shindo, P.W., Medina, F.R., Wicker, R.B.: Metal fabrication by additive manufacturing using laser and electron beam melting technologies. Journal of Materials Science & Technology **28**(1), 114 (2012). DOI 10.1016/S1005-0302(12)60016-4. 00059
36. Naelap, K., Veski, P., Pedersen, J.G., Anov, D., Jrgensen, P., Kristensen, H.G., Bertelsen, P.: Acoustic monitoring of a fluidized bed coating process. International Journal of Pharmaceutics **332**(12), 9097 (2007). DOI 10.1016/j.ijpharm.2006.09.036. 00030

37. Niri, E.D., Farhidzadeh, A., Salamone, S.: Adaptive multisensor data fusion for acoustic emission source localization in noisy environment. Structural Health Monitoring **12**(1), 5977 (2013). DOI 10.1177/1475921712462937. 00006
38. Peng, A., Xiao, X., Yue, R.: Process parameter optimization for fused deposition modeling using response surface methodology combined with fuzzy inference system **73**(1), 87–100 (2014-07-01). DOI 10.1007/s00170-014-5796-5. URL http://link.springer.com/article/10.1007/s00170-014-5796-5. 00000
39. Perez, A.R.T., Roberson, D.A., Wicker, R.B.: Fracture surface analysis of 3d-printed tensile specimens of novel ABS-based materials **14**(3), 343–353 (2014-06-01). DOI 10.1007/s11668-014-9803-9. URL http://link.springer.com/article/10.1007/s11668-014-9803-9. 00003
40. Q. Sun, G.M. Rizvi, C.T. Bellehumeur, P. Gu: Effect of processing conditions on the bonding quality of FDM polymer filaments **14**(2), 72–80 (2008-03-28). DOI 10.1108/13552540810862028. URL http://www.emeraldinsight.com/doi/full/10.1108/13552540810862028. 00044
41. Rao, P., Liu, J., Roberson, D., Kong, Z.J., Williams, C.: Online real-time quality monitoring in additive manufacturing processes using heterogeneous sensors. Journal of Manufacturing Science and Engineering (2015). DOI 10.1115/1.4029823. URL http://manufacturingscience.asmedigitalcollection.asme.org/article.aspx?doi=10.1115/1.4029823
42. Saude, N., Masood, S., Nikzad, M., Ibrahim, M., Ibrahim, M.H.I.: Dynamic mechanical properties of copper-abs composites for fdm feedstock. Int J Eng Res Appl **3**, 12571263 (2013). 00005
43. Sim, H.Y., Ramli, R., Saifizul, A.A., Abdullah, M.A.K.: Empirical investigation of acoustic emission signals for valve failure identification by using statistical method. Measurement **58**, 165174 (2014). DOI 10.1016/j.measurement.2014.08.028
44. Singh, R., Singh, S.: Development of nylon based fdm filament for rapid tooling application. Journal of The Institution of Engineers (India): Series C **95**(2), 103108 (2014). DOI 10.1007/s40032-014-0108-2
45. Sood, A.K., Equbal, A., Toppo, V., Ohdar, R.K., Mahapatra, S.S.: An investigation on sliding wear of FDM built parts **5**(1), 48–54 (2012). DOI 10.1016/j.cirpj.2011.08.003. URL http://www.sciencedirect.com/science/article/pii/S1755581711001040. 00009
46. Sood, A.K., Ohdar, R.K., Mahapatra, S.S.: Parametric appraisal of fused deposition modelling process using the grey taguchi method. Proceedings of the Institution of Mechanical Engineers, Part B: Journal of Engineering Manufacture **224**(1), 135145 (2010). DOI 10.1243/09544054JEM1565. 00016
47. Sood, A.K., Ohdar, R.K., Mahapatra, S.S.: Experimental investigation and empirical modelling of fdm process for compressive strength improvement. Journal of Advanced Research **3**(1), 8190 (2012). DOI 10.1016/j.jare.2011.05.001. 00010
48. Sun, J., Rahman, M., Wong, Y.S., Hong, G.S.: Multiclassification of tool wear with support vector machine by manufacturing loss consideration. International Journal of Machine Tools and Manufacture **44**(11), 11791187 (2004). DOI 10.1016/j.ijmachtools.2004.04.003. 00064
49. Sung Hoon Ahn, Michael Montero, Dan Odell, Shad Roundy, Paul K. Wright: Anisotropic material properties of fused deposition modeling ABS **8**(4), 248–257 (2002-10-01). DOI 10.1108/13552540210441166. URL http://www.emeraldinsight.com/doi/full/10.1108/13552540210441166. 00167
50. Teti, R., Jemielniak, K., ODonnell, G., Dornfeld, D.: Advanced monitoring of machining operations **59**(2), 717–739 (2010). DOI 10.1016/j.cirp.2010.05.010. URL http://www.sciencedirect.com/science/article/pii/S0007850610001976
51. Thrimurthulu, K., Pandey, P.M., Venkata Reddy, N.: Optimum part deposition orientation in fused deposition modeling. International Journal of Machine Tools and Manufacture **44**(6), 585594 (2004). DOI 10.1016/j.ijmachtools.2003.12.004. 00113
52. Turner, B.N., Gold, S.A.: A review of melt extrusion additive manufacturing processes: Ii. materials, dimensional accuracy, and surface roughness. Rapid Prototyping Journal **21**(3), 250261 (2015). DOI 10.1108/RPJ-02-2013-0017
53. Turner, B.N., Strong, R., Gold, S.A.: A review of melt extrusion additive manufacturing processes: I. process design and modeling. Rapid Prototyping Journal **20**(3), 192204 (2014). DOI 10.1108/RPJ-01-2013-0012

54. Vapnik, V.: The Support Vector Method of Function Estimation, p. 5585. Springer US (1998). 00202
55. Vapnik, V.: The Nature of Statistical Learning Theory. Springer Science & Business Media (2000). 00663
56. Wang, W., Ma, S., Fuh, J.Y.H., Lu, L., Liu, Y.: Processing and characterization of laser-sintered al2o3/zro2/sio2. The International Journal of Advanced Manufacturing Technology **68**(9-12), 25652569 (2013). DOI 10.1007/s00170-013-4863-7. 00001
57. Widodo, A., Yang, B.S.: Support vector machine in machine condition monitoring and fault diagnosis. Mechanical Systems and Signal Processing **21**(6), 25602574 (2007). DOI 10.1016/j.ymssp.2006.12.007. 00380
58. Wohlers, T.T.: Wohlers Report 2014: 3D Printing and Additive Manufacturing State of the Industry Annual Worldwide Progress Report. Wohlers Associates (2014). 00000
59. Xie, F., Wu, B., Hu, Y., Wang, Y., Jia, G., Cheng, Y.: A generalized interval probability-based optimization method for training generalized hidden markov model. Signal Processing **94**, 319329 (2014). DOI 10.1016/j.sigpro.2013.06.009. 00001
60. Yang, Z., Wu, H., Yu, Z., Huang, Y.: A non-destructive surface burn detection method for ferrous metals based on acoustic emission and ensemble empirical mode decomposition: from laser simulation to grinding process **25**(3), 035,602 (2014-03-01). DOI 10.1088/0957-0233/25/3/035602. URL http://iopscience.iop.org/0957-0233/25/3/035602. 00000
61. Yang, Z., Yu, Z., Wu, H., Chang, D.: Laser-induced thermal damage detection in metallic materials via acoustic emission and ensemble empirical mode decomposition. Journal of Materials Processing Technology **214**(8), 16171626 (2014). DOI 10.1016/j.jmatprotec.2014.03.009. 00000
62. Yao, Z., Mei, D., Chen, Z.: On-line chatter detection and identification based on wavelet and support vector machine. Journal of Materials Processing Technology **210**(5), 713719 (2010). DOI 10.1016/j.jmatprotec.2009.11.007. 00050
63. Ziemian, C., Sharma, M., Ziemian, S.: Anisotropic mechanical properties of ABS parts fabricated by fused deposition modelling. INTECH Open Access Publisher (2012). 00009